Environmental heterogeneity on landslide slopes affects the long-term recoveries of forest ecosystem components

Wataru Hotta[a], Junko Morimoto[a], Seiji Yanai[b], Yoshitaka Uchida[c], Futoshi Nakamura[a]

[a] Ecosystem Management Laboratory, Graduate School of Agriculture, Hokkaido University, Sapporo 060-8589, Japan

[b] Division of Sciences for Bioproduction and Environment, Ishikawa Prefectural University, Nonoichi 921-8836, Japan

[c] Environmental Biogeochemistry Laboratory, Graduate School of Agriculture, Hokkaido University, Sapporo 060-8589, Japan

Corresponding author: W. Hotta

E-mail: w-hotter97thank-you@eis.hokudai.ac.jp

Tel: +81-11-706-2522

Postal Address: Graduate School of Agriculture, Hokkaido University, Kita 9, Nishi 9, Kita ku, Sapporo, Hokkaido 060-8589, Japan

Highlights

- Rich landslide legacies and low slope angles promoted vegetation and soil recovery
- Legacy richness and timing of canopy closure determined changes in the understory
- Landslide mortality and stand development mortality determined changes in dead wood

Abstract

Landslides are a common disturbance in mountainous areas of the world. Transporting and accumulating landslide debris, i.e., disturbance legacies, such as coarse woody debris (CWD), vegetation patches, and surface soils, generate a heterogeneous environment along slopes (zones), which are suggested to affect forest recovery. However, the long-term changes in forest ecosystems after landslides remain unknown, particularly zone-dependent change patterns. We aimed to reveal the differences in the changes in live trees, understory vegetation, CWD, and soils among zones by surveying forests with landslide ages (years since the landslide) ranging from 3 to 74 years and reference stands. The increase in live tree aboveground biomass occurred at a faster rate at the lower part of the slopes where the disturbance legacies were rich and surface soils were stabilized due to the smaller slope angle. Chronological patterns of understory vegetation amounts were determined by the differences in disturbance legacy richness and the timing of subsequent canopy closure. The amounts and decay-class diversity of CWD were determined by the differences in legacy richness and mortality through stand development. These zone-dependent chronological changes influenced litter production and determined the recovery rates of surface soil carbon and nitrogen stocks. The increase in the dominance rates of forest herbaceous species was faster in the lower part of the slopes due to the faster surface soil development and canopy closure. Our results illustrate that long-term forest ecosystem succession and recovery after landslides occurs more rapidly at the lower parts than at the upper parts of slopes.

Keywords

slope failure; biological legacy; soil erosion; dead wood; forest floor; soil nutrient

1. Introduction

Natural disturbances are one of the major factors shaping forest ecosystems by affecting forest structure, composition, and functional processes, such as plant growth, mortality, and decomposition of litter and soils (Dale et al., 2001). Once forests are profoundly disturbed, several processes in forest ecosystems are altered, e.g., massive live tree die-off, changes in plant species composition due to improvement of light conditions, increasing decomposition rates of CWD and soils (Zhang and Liang, 1995). Forest ecosystem components, such as live trees, coarse woody debris (CWD), understory vegetation, and soils, are interacting with each other via several processes such as litter fall and decomposition, and seed dispersal and seedling growth. Therefore, recoveries of these multiple ecosystem components need to be evaluated to understand forest ecosystem recovery after disturbances.

Post-disturbance recovery rates of forest structure and functions such as stand basal area and carbon dynamics vary widely depending on disturbance types (Amiro et al., 2010; Bartels et al., 2016). In many studies, the recoveries of multiple forest ecosystem components after wildfire, windthrow, insect outbreak, or harvest have been evaluated (e.g., Hansen et al., 2015; Hotta et al., 2020; Rothstein et al., 2004; Seedre et al., 2014). However, studies focusing on forest recovery after landslides, which are one of the major natural disturbances in mountainous areas of the world (Restrepo et al., 2009), are understudied. Landslides are predicted to occur more frequently and intensely in the future because of the increase in heavy rain events, which is the major trigger of shallow landslides attributable to climate change (Lateltin et al., 1997). Thus, there is an urgent need to understand forest ecosystem recovery after landslides.

Landslide events shape relatively distinct zones by transporting and accumulating undisturbed vegetation patches, CWD, and soils, which cause heterogeneity of recovery rates of forest ecosystem components. Generally, each landslide is divided into three zones from top to bottom: the initiation zone, the transport zone, and the deposition zone (Restrepo et al., 2009; Walker et al., 2009). Each zone is characterized by the amount of disturbance legacy (i.e., undisturbed vegetation patches, soils and CWD transported from the upper part to the lower part of slopes; Johnstone et al., 2016) and the physical environment, such as slope angle and soil fertility (Walker et al., 2009). Because of this heterogeneity, previous studies suggested that tree, herb, and soil recoveries would be slower on the upper parts of slopes because of lower soil stabilities and fertilities due to higher slope angles (Buma and Pawlik, 2021; Guariguata, 1990; Wilcke et al., 2003).

We still do not have enough knowledge about the differences in the long-term changes in multiple forest ecosystem components among the zones generated by landslides. Previous studies focusing on the entire landslide scars (i.e., not considering the zones) reported that it takes more than 25 to 120 years for stand basal area recovery (Pandey and Singh, 1985; Reddy and Singh, 1993; Restrepo et al., 2003), and 35 to 120 years for soil carbon and nitrogen recovery (Pandey and Singh, 1985; Reddy and Singh, 1993). However, these studies could not capture the spatial heterogeneity of recovery within landslides. Moreover, previous studies considering zones (e.g., Guariguata, 1990; Wilcke et al., 2003) focused on a single ecosystem component or on short-term (less than 10 years) responses of ecosystems, although several decades to hundred years are needed for forest development, and ecosystem recovery should be evaluated by investigating the dynamics of multiple ecosystem components.

This study aimed to reveal how the long-term (over 70 years) change patterns of (1) the amount of multiple forest ecosystem components and (2) those of species composition after shallow landslides differed among the zones generated by landslides. We hypothesize that the recovery rates of live tree aboveground biomass (AGB), surface soil carbon and nitrogen stocks (CN) and succession of species composition occur at a faster rate in the deposition zone than the transport and the initiation zones due to the richer disturbance legacies and the soil stability at the lower slope angle positions. Additionally, we hypothesize that the chronological changes in the amounts of understory vegetation and CWD are different among the zones due to differences in the amounts of disturbance legacies remaining and the subsequent stand development.

2. Materials & Methods

2.1 Study area

The study area was located in mixed forests in the transition zone of the cool-temperate and boreal areas in southern Hokkaido, northern Japan (Fig. 1). The annual mean temperature and precipitation are 7.0 °C and 1,028.4 mm, respectively, at the meteorological observation station in Atsuma (42°43′48″N, 141°53′18″E; at 20 m a.s.l.), and 7.6 °C and 983.7 mm, respectively, at the meteorological observation station in Hidaka-Monbetsu (42°29′48″N, 142°3′12″E; at 47 m a.s.l.) (Japan Meteorological Agency, 2022; average of 1991-2020). The altitude above sea level is 47 to 221 m. Because of the low temperature (below 0 °C) and relatively thin snow cover (21-69 cm at maximum) during winter, freeze-thaw action causes soil instability. The dominant parent material consists of Tertiary mudstone and conglomerate, Quaternary terrace deposits, volcanic ash, and pumice (Geological Survey of Japan, 2022). The dominant soil types are Andosols and partly volcanogenous Regosol (IUSS Working Group WRB, 2015). The forest canopy around landslides is dominated by cool-temperate broadleaves such as *Tilia japonica* (Miq.) Simonk, *Acer pictum* Thunb., and *Quercus crispula* Blume var. *crispula*.

2.2 Sampling design

We used chronosequence approaches to estimate the long-term forest ecosystem changes. First, we chose five landslides for each landslide age (years since the landslide; 3, 18, 40, and over 74 years post-landslides; i.e., landslides occurred in 2018, 2003, 1981, and before 1947) and three reference stands that are considered not to experience catastrophic disturbances since 1947 and no evidence of disturbances was observed in the aerial photographs taken in 1947. The areas of landslides ranged from 0.05 to 0.7 ha. We selected suitable landslides and stands (Fig. 1) by reviewing the time series of aerial photographs and the records of previous studies (Sato et al., 2013; Yanai and Igarashi, 1990).

Next, we divided each landslide or stand into three zones: initiation, transport, and deposition for landslides (Restrepo et al., 2009; Walker et al., 2009) and upper, middle, and lower for reference stands (Figure S1.1, S1.2, S1.3, and S1.4). The initiation zone is the starting point of landslides and is characterized by a steep slope and infertile soils; the deposition zone is the end part of landslides and legacies, which existed on slopes, are accumulated here; and the transport zone is the transition zone between the initiation and deposition zones (Walker et al., 2009). Because it is difficult to distinguish among the zones in the field, particularly for old landslides, we determined zones as follows by reviewing aerial photos and vector polygon files: the initiation and transport zones were defined as the upper and lower half of a landslide scar, respectively, and the deposition zone was defined as the area adjacent to the landslide scar at the bottom of the slope. We reviewed aerial photos taken in 1947 and 1983 to identify zones in landslides that occurred before 1947 and in 1981, respectively. We reviewed vector polygon files created by reviewing aerial photos (Kita, 2018; Sato et al., 2013) to identify zones in landslides that occurred in 2003 and 2018.

2.3 Field data collection

In each zone, we first established one plot of 15 m × 15 m for surveying living trees with a height larger than 1.3 m and CWD. When the area of a zone was smaller than 225 m^2, the whole zone was surveyed. Second, we established four quadrats of 2 m × 2 m for surveying soil moisture content, slope angle, O layer depth, and the understory vegetation, which included all nontree vascular plants and trees with a height smaller than 1.3 m. Last, we established one quadrat of 0.25 m × 0.25 m for sampling organic (O) layer and mineral soils. Originally, the three zones are transitive and boundaries among zones are ambiguous. Thus, we established plots in the center part of each zone rather than near boundaries to robustly investigate differences in the recovery of forest ecosystems among zones. We could not establish plots and quadrats in the deposition zone of landslides over 74 years ago because roads and farmland were newly built in their deposition zones, and we could not find suitable survey areas.

For the living trees with a height larger than 1.3 m, we recorded species and measured the diameter at breast height (DBH) with a tree caliper (when DBH was larger than 46 cm, it was measured with a measuring tape) and tree heights with a TruPulse 360 rangefinder (Laser Technology Inc., USA). For the understory vegetation, we identified species and measured the coverage and the maximum height of each species.

We classified CWD according to three types and five-level decay classes. CWD included snags, downed logs, and stumps. Snags are standing dead trees taller than 1.5 m. Downed logs are dead trees that lay on the ground and did not have roots and that lay on the ground with roots and stems longer than or equal to 1.5 m. Stumps are standing dead trees shorter than 1.5 m and dead trees laying on the ground with roots and stems shorter than 1.5 m (Forestry and Forest Products Research Institute, 2016). Snags with DBHs larger than 5 cm were targeted for recording whether conifers or broadleaves and the decay class and measuring DBH and heights. Downed logs with the diameter of either end larger than 10 cm were targeted for recording whether conifers or broadleaves and the decay class and measuring diameters of both ends and lengths. We targeted stumps with a diameter of the upper end larger than 5 cm; however, no such stumps were observed in any of the plots. We used the five-level decay classification system (i.e., I, II, III, IV, and V, where I is the newest and V is the oldest) described in Graham and Cromack (1982). The decay class of CWD was identified based on the morphological characteristics and the depths of the knife sticks (Fukasawa, 2012; Heilmann-Clausen, 2001).

Soil moisture content, slope angle, and O layer depth were measured. Time domain reflectometry (HydroSense, Campbell Scientific, Inc.) was used to measure the water content of the soil by volume. The soil water content was measured on a day following three continuous sunny days in mid-October 2021 and measured four times at 5 cm beneath the surface in each quadrat. The growing season of our study site ranges from May to October (Wang et al., 2004). The slope angle and O layer depth were measured at the center of each quadrat.

We sampled the O layer and mineral soils in 0.25 m × 0.25 m quadrats. We classified the O layer into the Oi layer, the Oa/Oe layer (the Oi layer contains fresh leaf litter, but the Oa/Oe layer contains well-decomposed litter), and twigs and then sampled all of the O layer within the quadrats. We sampled the surface mineral soils (0-5 cm depth) below the O layer in each quadrat by using cylindrical cores (100 mL) and measured the bulk density. We also sampled approximately 200 g of surface mineral soils (0-5 cm depth) by shovels to analyze the carbon and nitrogen concentrations.

All surveys were conducted from July to October 2021.

2.4 Soil analysis

The O layer samples were dried in an oven (70 °C, 48 h), and their dry weights were measured. Then, we finely ground them by using a Wiley mill (W-100S, IRIE SHOKAI Co., Ltd., Japan) and a ball mill (Sample Mill TI-100, CMT Co., Ltd., Japan). Finally, the carbon and nitrogen concentrations of each sample were measured using a CHNS/O analyzer (PE-2400, PerkinElmer, USA).

Mineral soil samples for measuring bulk densities were dried, and we classified each mineral soil sample for measuring bulk density into fine soil particles, gravel, and roots by passing them through a 2 mm sieve. After drying, the dry weight of the fine soil was measured. The bulk density was calculated according to the dry weight of fine soils divided by the volume (i.e., 100 mL).

The mineral soils collected for measuring carbon and nitrogen concentrations were air dried and then passed through a 2 mm sieve followed by a 500 μm sieve. The carbon and nitrogen concentrations of each sample were also measured using the CHNS/O analyzer (PE-2400, PerkinElmer, USA).

2.5 Data analysis

2.5.1 Calculations of live tree AGB, CWD mass, the biomass index of understory vegetation, and slope aspect

Live tree AGB was calculated using species-specific equations. Downed log mass was calculated using the conic-paraboloid formula (Fraver et al., 2007) and the decay class specific volume density. Snag mass was calculated by approximating their shape to cones. Please see supplementary material S2 for details on the mass calculations. The biomass index of the understory vegetation was calculated as the sum of the coverage of each species (decimals ranging from 0.0 to 1.0) multiplied by the maximum height of each species (cm) (Suchar and Crookston, 2010).

We calculated slope aspect as follows. First, we calculated azimuths which slopes are facing based on a 10-m resolution digital elevation model by using QGIS version 3.18.2 (QGIS

Development Team, 2021). Next, we calculated slope aspect as a following equation according to Chang et al. (2006): 180 − | azimuth − 180 |. Slope aspect varies from 0 (north-facing slopes) to 180 (south-facing slopes).

2.5.2 Statistical analysis

Differences in slope angle, the O layer depth, soil moisture content, live tree AGB, CWD mass, the biomass index of understory vegetation, surface soil carbon and nitrogen stocks, including the O layer and mineral soils among landslide ages and zones, were tested with a generalized linear mixed model (GLMM; *lme4* package) and multiple comparisons (*multcomp* package; *p* adjustment methods: Benjamini–Hochberg method (Benjamini and Hochberg, 1995)). The values of soil moisture content, live tree AGB, CWD mass, and the biomass index of understory vegetation were natural logarithm-transformed to improve normality and homogeneity of variances of residuals. The explanatory variable was the combination of landslide ages and zones. The error terms were assumed to follow a gamma distribution for O layer depth and a normal distribution for the other variables. The random effect was the landslide identity for GLMMs of live tree AGB, CWD mass, and surface soil carbon and nitrogen stocks. Regarding the GLMM of the biomass index of understory vegetation, slope angle, the O layer depth, and soil moisture content, the random effects were the landslide identity and the plot identity. We ran eight GLMMs in total.

We used two complementary statistical analyzes on a site-species matrix to examine variation of species composition among sites. First, we used the permutational analysis of variance (PERMANOVA; *vegan* package (Oksanen et al., 2022)) and multiple comparisons (*pairwiseAdonis* package (Martinez Arbizu, 2020)) to test dissimilarities in the species composition of living trees and understory vegetation. The explanatory variable was the combination of landslide ages and zones. The response variables were the plot-species matrix of the basal area for living tree species composition and the quadrat-species matrix of the vegetation cover (2/pi*arcsin(sqrt(x)) transformed) for understory vegetation species composition. Second, the non-metric multidimensional scaling (NMDS) was conducted to visualize differences in species compositions among the combinations of landslide ages and zones and to identify environmental factors determining species compositions (*vegan* package (Oksanen et al., 2022)). We considered two geomorphic variables (i.e., slope angle and slope aspect), four soil variables (i.e., soil moisture content, surface soil carbon and nitrogen stocks, and O layer depth) to explain patterns in species composition. For the understory analysis, AGB was additionally considered. If the p value was lower than 0.05 in the analysis using the function *envfit*, then we regarded the relevant factor as the determining factor of species compositions. Note that the plots in landslide ages 3 and 18 were excluded from analyses of live tree species composition because of the low number of individuals.

In all analyzes, we set one variable of the combination of landslide ages and zones as an explanatory variable rather than treat landslide ages and zones independently because of the incomplete design due to the lack of data of the deposition zone in landslides over 74 years. All statistical analyses were conducted in R 4.2.2 (R Core Team, 2022). Additionally, we classified live tree species by shade and desiccation tolerance. Herbaceous species were classified into three species types, i.e., open land species, generalist species, and forest species, and three moisture types, i.e., dry, moderate, and wet.

3. Results

3.1 Environmental characteristics and forest ecosystem components

3.1.1 Environmental characteristics of landslide ages and zones

The differences in slope angles were mainly explained by zones because slope angles were significantly different among the zones for almost all landslide ages (Table 1). The differences in O layer depths were mainly explained by landslide age; however, significant differences among the zones were observed for landslide age 18 (Table 1). The differences in soil moisture contents were mainly explained by zones (Table 1).

3.1.2 Initial ecosystem conditions after the landslide

The amounts of understory vegetation and CWD were significantly larger in the deposition zone than in the initiation and transport zones with landslide age 3, which is the earliest age after a landslide in this study (Table 2). Live tree AGB and surface soil CN were not significantly different among the zones.

3.1.3 Live trees

Live tree AGB increased regardless of zone; however, the increase in AGB was slower in the initiation zone than in the other zones (Fig. 2a). AGB 40 years after landslides in the initiation zone was significantly lower than those in the transport and deposition zones ($p < 0.05$). AGB over 74 years after landslides was marginally significantly different between the initiation and transport zones ($p < 0.10$). Additionally, AGB over 74 years after landslides was significantly lower in the initiation zone ($p < 0.05$) and marginally significantly lower in the transport zones ($p < 0.10$) from those in the reference stands.

3.1.4 Understory vegetation

Each zone had unique patterns of chronological changes in the biomass indices of understory vegetation. Unimodal distributions with peaks at 18 and 40 years after landslides were observed in the transport and initiation zones, respectively (Fig. 2b, center and left). Biomass indices in the deposition zone were largest at 3 years after landslides and decreased with years elapsed (Fig. 2b, right). In addition, the biomass indices 3 years after landslides in the deposition zone were significantly larger than those in the initiation and transport zones ($p < 0.05$). The biomass indices 18 years after landslides in the transport and deposition zone were significantly larger than those in the initiation zone ($p < 0.05$).

3.1.5 CWD

The chronological changes in CWD mass also had unique patterns dependent on zone. The CWD mass at the initiation zone was largest in the reference stands and monotonically increased with landslide age (Fig. 2c, left). U-shaped chronological changes in CWD mass with peaks at 3 years after landslides and reference stands were observed in the deposition zone (Fig. 2c, right). A similar pattern was also observed in the transport zone, although there were no significant differences with time after landslide (Fig. 2c, center). In addition, the CWD mass 3 years after landslides was significantly larger in the deposition zone than in the initiation and transport zones. Chronological changes in CWD decay class compositions were also different among zones (Fig. 2c). CWD in decay classes III, IV, or V was observed in the transport and deposition zones in areas 18 or more years after landslides; however, these classes were not observed in the initiation zone unless it was more than 74 years after landslides.

3.1.6 Surface soils

The recovery rates of surface soil CN were different among the zones. In the initiation and transport zones, surface soil CN at 40 and over 74 years after landslides were not significantly different from those in the reference stands; thus, surface soil CN recovered to their reference levels within 40 years after landslides (Fig. 2d and e, left and center). In the deposition zone, the surface soil CN 18 years after landslides were not significantly different from those in the reference stands, thus recovering to their reference levels within 18 years after landslides (Fig. 2d and e, right). Additionally, the surface soil CN 18 years after landslides were significantly larger in the deposition zone than in the initiation and transport zones ($p < 0.05$). Both carbon and nitrogen stocks showed similar patterns of temporal changes.

3.2 Species composition

3.2.1 Live tree species composition

The species composition of live trees showed different trends among landslide ages and zones. Although, live tree species composition was not significantly different among the landslide ages regardless of zones according to PERMANOVA (Fig. 3c), the NMDS ordination result and the dominance rate of the basal area showed some differences in species composition (Fig. 3a, c, and d). Regardless of zones, shade-intolerant species tended to be most dominant in the landslide age 40. Plots at landslide age 40 were characterized by shade-intolerant species such as *Betula platyphylla* and *Alnus hirsuta*; however, plots at landslide age ≥ 74 and the reference were characterized by intermediate and shade tolerant species such as *Acer pictum*, *Quercus crispula*, and *Tilia japonica* (Fig. 3a and b). These tendencies were also clearly recognized the dominance rate of the basal area (Fig. 3c). Desiccation-intolerant species tended to be most dominant in the order of the deposition, transport, and initiation zones (Fig. 3a, b, and d). Regardless of landslide age, the NMDS results showed that plots in the deposition zone were characterized by desiccation-intolerant species such as *Alnus hirsuta*, *Carpinus cordata*, *Ulmus davidiana* var. *japonica*, and *Cercidiphyllum japonicum* (Fig. 3a and b). Desiccation-intolerant species accounted for more than 50% of the total basal area in the deposition/lower zone regardless of landslide age (Fig. 3d). The slope angle (r^2 = 0.338, p = 0.001), soil moisture content (r^2 = 0.287, p = 0.004), and surface soil nitrogen stock (r^2 = 0.244, p = 0.014) were significantly correlated to the ordination results (Fig. 3a and S4). Surface soil carbon stock (r^2 = 0.174, p = 0.0524) was marginally significantly correlated to the ordination results (Fig. 3a and S4). O layer depth (r^2 = 0.092, p = 0.233) and slope aspect (r^2 = 0.084, p = 0.244) were not significantly correlated to the ordination results (Fig. 3a and S4). The surface soil carbon and nitrogen stocks were suggested to mainly indicate the environmental differences among landslide ages, while the soil moisture content and slope angle were suggested to mainly indicate the environmental differences among zones.

3.2.2 Understory vegetation species composition

Understory vegetation species composition was significantly different among the landslide ages and zones according to PERMANOVA and NMDS (Fig. 4a, b, c, and d). Quadrats with younger landslide ages were characterized by open land species and species that favor dry environments; however, quadrats with older landslide ages were characterized by forest species (Fig. 4a, b, c, and d). The dominance rate of vegetation cover also showed a decrease in open land species and an increase in generalist and forest species with increasing landslide age (Fig.

4e). In particular, the dominance rate of forest species cover increased more rapidly, and the dominance rate of open land species cover decreased more rapidly in the deposition zone than in the initiation zone (Fig. 4e). The dominance rate of forest species cover in the deposition zone 18 years after landslides was 45%, which was approximately three times that in the initiation zone, i.e., 16% (Fig. 4e). The dominance rate of open land species cover in the deposition zone 18 after landslides was 17%; however, that in the initiation zone was 28% (Fig. 4e). Regardless of landslide ages (except for age 3), quadrats in the deposition/lower zones were characterized by species that favor moist environments (Fig. 4c and d), and the dominance rate of this type of species cover was larger in the deposition/lower zone than in the initiation/upper and transport/middle zones (Fig. 4f). AGB ($r^2 = 0.366$, $p < 0.001$), slope angle ($r^2 = 0.028$, $p = 0.026$), soil moisture content ($r^2 = 0.065$, $p < 0.001$), O layer depth ($r^2 = 0.576$, $p < 0.001$), surface soil carbon stock ($r^2 = 0.501$, $p < 0.001$), surface soil nitrogen stock ($r^2 = 0.449$, $p < 0.001$), and slope aspect ($r^2 = 0.076$, $p < 0.001$) were significantly correlated to the ordination results (Fig. 4a, b, c and S5). AGB, surface soil carbon and nitrogen stocks, and O layer depth mainly indicated the environmental differences among landslide ages. Additionally, the soil moisture content and slope angle mainly indicated the environmental differences among zones.

4. Discussion

We analyzed the long-term changes in multiple forest ecosystem components in three zones generated by landslides. As we hypothesized, the recovery rates of live tree AGB and soil CN were faster in the deposition zone than the transport and the initiation zones. The chronological changes in the amounts of understory vegetation and CWD were also different among the zones. Additionally, zone-dependent environment affected species composition and the succession of understory species composition was faster at lower part of slopes. However, in contrast to our hypothesis, the succession of live trees species composition did not significantly differ among zones. In the following, we discuss the drivers of zone-dependent recoveries of forest ecosystem components and species composition.

4.1 Chronological changes in the amount of forest ecosystem components

Live tree AGB recovery was facilitated by the low slope angle and disturbance legacy richness. The slope angle was greatest in the initiation zone, followed by the transport zone and then the deposition zone (Table 1). More surface soils are eroded and lost on steep slopes due to rainfall (Martínez-Murillo et al., 2013; Warrington et al., 1989). Thus, surface soils in the initiation zone were less stable than those in the transport and deposition zones, and it was more difficult for tree seedlings to establish, particularly during several years just after landslides (Buma and Pawlik, 2021; Guariguata, 1990). Moreover, needle ice forms and melts in soils during the winter season in the cool-temperate climate regions where our study sites were located, and this process destabilizes surface soils and facilitates soil erosion (Prosser et al., 2000). Thus, this factor may have been a why live tree recovery in the present study was slower than that in warmer climate regions as reported in previous studies (Joshi and Garkoti, 2021; Schomakers et al., 2017).

Disturbance legacies (i.e., undisturbed vegetation patches and CWD) were richest in the deposition zone, followed by in the transport zone and then the initiation zone (Table 2) because they were transported from the upper part of slopes when shallow landslides occurred. The amounts of CWD and understory vegetation 3 years after landslides were much larger in the deposition zone than in the initiation and transport zones (Table 2), which directly indicated that the amounts of disturbance legacy were larger in the deposition zone, although the understory vegetation in this zone 3 years after landslides contained some newly dispersed and established vegetation after the landslides. At disturbance legacy-rich sites, live trees can regenerate by advanced seedlings on undisturbed vegetation patches, buried seeds, or sprouts (Guariguata, 1990). Freund et al. (2021) also suggested that canopy heights are higher for 25 years after landslides at sites that include residual vegetation. Therefore, the accumulation rates of live tree AGB were highest (Fig. 2a) in the deposition zone, followed by the transport zone and then the initiation zone. Supplementary, live tree recovery after shallow landslides was relatively slower than that of the other disturbance types. Please see supplementary material S7 for a detailed discussion.

Disturbance legacy richness, slope angles, and timing of canopy closure associated with stand development determined the chronological patterns of understory vegetation amounts dependent on zones. The understory vegetation biomass index 3 years after landslides was larger in the deposition zone than in the other two zones (Table 2; Fig. 2b, landslide age 3), which could be attributed to the richness of undisturbed vegetation patches, buried seeds, rhizomes and the lower slope angle, as discussed above. In particular, species that reproduce via rhizomes, such as dwarf bamboo (*Sasa*) and *Petasites japonicus* subsp. *Giganteus*, may have assisted in rapid vegetation recovery (Hind and Kay, 2006; Makita et al., 1993). However, in the initiation and transport zones, seed dispersal and establishment were needed for vegetation recovery, and surface soils were exposed to soil erosion, as mentioned above; thus, the vegetation recovery was slower than that in the deposition zone.

The canopy closure associated with the increase in live tree AGB caused the understory vegetation biomass indices to finally decrease regardless of zone (Fig. 2b). Jules et al. (2008) suggested that the amount of understory vegetation gradually decreases with stand development in first 100 years after stand-replacing disturbances. Live tree AGB accumulated more slowly in the initiation zone than in the other two zones (Fig. 2a), which suggests that canopy closure occurred later in the initiation zone. Therefore, biomass indices began to decline 40 to 74 years after landslides in the initiation zone, which was later than that in the deposition zone.

The chronological patterns of the CWD amounts were determined mainly by the loss and accumulation of CWD due to landslides and the additional input of CWD through subsequent stand development. Once landslides occurred, live trees and CWD on the slope were transported to and accumulated at the lower part of the slope (landslide mortality, which partially includes carryover). In fact, our data also showed an uneven distribution of CWD on the slopes just after landslides, i.e., more CWD in the deposition zone and less CWD in the initiation and transport zones (Table 2; Fig. 2c, landslide age 3). These unevenly distributed CWD was decomposed, which likely resulted in differences in the amounts of decayed CWD (decay class III, IV, or V) among the zones 18 and 40 years after landslides (Fig. 2c). Regardless of zone, the amount of CWD eventually tended to increase due to the increase in mortality by self-thinning through stand development (Yoda et al., 1963). Therefore, the combination of mortality due to landslides and the CWD input from the new stand determined the chronological patterns of the CWD amount in each zone. Thus, the chronological changes in CWD in the initiation zone showed only CWD input from the new stand, while those in the transport zone showed a few CWD input by landslides and CWD input from the new stand; finally, those in the deposition zone showed a lot of CWD input by landslides and CWD input from the new stand, which was a “U-shaped temporal pattern” (Spies et al., 1988). U-shaped temporal patterns were also reported in previous studies focused on other disturbance types, such as wildfire, windthrow, and harvest (Brassard and Chen, 2008; Krankina and Harmon, 1995; Spies et al., 1988). Unlike other disturbance types, landslides generate chronological patterns of CWD amounts that can be completely different within disturbed areas.

The recovery rates of surface soil CN dependent on zones were determined by the difference in slope angles and the amounts of litter, which was induced by both the amounts of CWD just after the landslides and the recovery rates of understory vegetation and live trees. As we have discussed above, more soils eroded on the upper part of the slopes; thus, soil development was relatively slow in the upper part of the slopes. Additionally, the accumulation rates of understory vegetation and live tree AGB were the fastest in the deposition zone, followed by the transport zone and then the initiation zone (Fig. 2a, b, c). These results suggest that the amounts of litter of both understory vegetation and live trees were also greatest in the deposition zone, followed by the transport zone and then the initiation zone. In forest ecosystems, litter fall is one of the main sources of soil carbon and nitrogen. Additionally, the amounts of CWD just after the shallow landslide events were also largest in the deposition zone, followed by the transport zone and then the initiation zone. This leaf and wood litter is decomposed and transferred to surface soils. Thus, the surface soil CN recovered to the level of the reference stands faster in the deposition zone (18 years), followed by the transport zone (18-40 years) and then the initiation zone (40 years) (Fig. 2d and e and S6). Wilcke et al. (2003) also reported that the accumulation of soil nutrients occurred more rapidly at the lower part of landslides within 20 years.

Regardless of zone, surface soil CN recovered to the level of reference stands faster than the recovery of live tree AGB, which took more than 74 years. Previous studies have also reported a faster recovery of surface soil CN than of live trees (Pandey and Singh, 1985; Reddy and Singh, 1993). Because soil nitrogen is one of the most important factors for plant succession and tree growth (Shiels et al., 2008; Walker et al., 2009) , surface soil CN recovery rates might influence deeper soil CN recovery and long-term (over 100 years) live tree AGB recovery, which was beyond the scope and timescale of the present study.

4.2 Chronological changes in live tree and understory vegetation species composition

Landslide age- and zone-dependent environmental conditions are suggested to affect live tree and understory vegetation species composition. Higher surface soil carbon and nitrogen stocks and O layer depth (Fig. 3a and 4a, b, and c), which were greatly correlated with landslide ages and partly correlated with zones (Fig. 2e; Table 1), resulted in shade-tolerant species and forest species dominance among the live trees and understory vegetation, respectively. Particularly, soil carbon and nitrogen are important for sustaining soil fertility (Lal, 2004; Vitousek and Howarth, 1991). Shade-tolerant species are often large-seeded species (Reich et al., 1998), and Jager et al. (2015) suggested that large-seeded shade-tolerant species favor high-fertility soils. Thus, the soil carbon and nitrogen stocks and O layer depth coupled with years elapsed after shallow landslides would facilitate shade-tolerant species and forest species dominance. Increasing AGB, which would positively correlate canopy closure associated with landslide age, significantly affected the understory vegetation species composition. Live tree AGB recovery occurred most rapidly in the deposition zone, followed by the transport zone and then the initiation zone, due to the low soil erosion levels and rich biological legacies in the deposition zone, as discussed above. Thus, species composition succession of understory vegetation occurred fastest in the deposition zone, followed by the transport zone and then the initiation zone.

Significant effects of soil moisture content and slope angle (Fig. 3a; Fig. 4a, b, c, and d), which were higher and smaller in order of the deposition, transport, and initiation zones (Table 1), suggested the presence of zone effects on the species composition of live trees and understory vegetation, although there were no significant differences in live tree species composition among the zones. In general, the deposition zones were located along or above streams (Fig. S1.1, S1.2, S1.3, and S1.4) because debris generated by landslides continues downward until it reaches flat terrain or a valley. Thus, forests such as riparian forests then developed, and species that favor moist environments were dominant in the deposition zones. Slope aspect would explain a variation in environment among sites not associated with landslide ages or zones. North-facing slopes (low slope aspect) are characterized by moister conditions compared to south-facing slopes (high slope aspect) (Boerner, 2006). This type of environment likely promotes the dominance of mesophytic plant species (Murphy et al., 2015), which is consistent with our results.

5. Conclusions

In this study, we analyzed how the long-term change patterns of the amount of multiple forest ecosystem components and those of species composition after shallow landslides differed among the zones generated by landslides. As we hypothesized, the accumulation of live tree AGB was slower in the initiation zone than in the other zones, as disturbance legacies in the initiation zone were minimal and surface soils were destabilized due to the higher slope angle. The chronological changes in the amounts of understory vegetation were determined by the difference in the amounts of disturbance legacies just after a landslide and the timing of subsequent canopy closure, which was dependent on zones. For the same reason, the succession of understory vegetation species composition occurred most rapidly in the deposition zone, followed by in the transport zone and then the initiation zone. The chronological changes in the amounts of CWD were determined by the difference in the amounts of disturbance legacies just after a shallow landslide and mortality through stand developments. Furthermore, zone-dependent chronological changes in live trees, understory vegetation, and CWD influenced subsequent litter production and determined the recovery rates of surface soil CN. With concerns about the increasing frequency and intensity of shallow landslide events under climate change, our results contribute to a detailed understanding of the response of forest ecosystems to shallow landslides.

CRediT author statement

Wataru Hotta: Conceptualization, Methodology, Formal analysis, Investigation, Data curation, Writing – Original Draft, Writing – Review & Editing, Visualization, Project administration, Funding acquisition. **Junko Morimoto**: Conceptualization, Methodology, Writing – Review & Editing, Supervision, Funding acquisition. **Seiji Yanai**: Methodology, Resources, Writing –

Review & Editing. **Yoshitaka Uchida**: Methodology, Resources, Writing – Review & Editing. **Futoshi Nakamura**: Writing – Review & Editing.

Funding

Funding for this study was supported by a KAKENHI grant from the Japan Society for the Promotion of Science (Grant Number 21J21458 and 22H02372).

Declaration of Competing Interest

The authors declare that they have no known competing financial interests or personal relationships that could have appeared to influence the work reported in this paper.

Data statement

Data is available on Dryad: https://datadryad.org/stash/share/0cVLSf5uOq-CE3xeuDUIy7FbFgUrMibs85Ub57uR-Y8

Acknowledgments

We thank the members of the Ecosystem Management Laboratory for helping with the field survey and for their helpful discussions about our study. We thank Ms. Yuriko Horiuchi, Ms. Akari Kimura, Dr. Takahiro Inoue, Dr. Hayato Maruyama and Dr. Toshihiro Watanabe for helping with the soil analysis. We thank Dr. Hajime Sato for allowing us to use data of historical landslides, Dr. Satoshi N. Suzuki and Dr. Kazuhiro Kawamura for helpful advice about statistical analysis, and Dr. Takashi Yamada for valuable advice on the study design. We would like to thank Atsuma town, Hidaka town, Biratori town, and the other subjects which own forest area of

plots, for allowing us to study these sites.

References

Amiro, B.D., Barr, A.G., Barr, J.G., Black, T.A., Bracho, R., Brown, M., Chen, J., Clark, K.L., Davis, K.J., Desai, A.R., Dore, S., Engel, V., Fuentes, J.D., Goldstein, A.H., Goulden, M.L., Kolb, T.E., Lavigne, M.B., Law, B.E., Margolis, H.A., Martin, T., McCaughey, J.H., Misson, L., Montes-Helu, M., Noormets, A., Randerson, J.T., Starr, G., Xiao, J., 2010. Ecosystem carbon dioxide fluxes after disturbance in forests of North America. J. Geophys. Res. 115, G00K02. https://doi.org/10.1029/2010JG001390

Bartels, S.F., Chen, H.Y.H., Wulder, M.A., White, J.C., 2016. Trends in post-disturbance recovery rates of Canada's forests following wildfire and harvest. For. Ecol. Manage. 361, 194–207. https://doi.org/10.1016/j.foreco.2015.11.015

Benjamini, Y., Hochberg, Y., 1995. Controlling the False Discovery Rate: A Practical and Powerful Approach to Multiple Testing. J. R. Stat. Soc. Ser. B 57, 289–300. https://doi.org/10.1111/j.2517-6161.1995.tb02031.x

Boerner, R.E.J., 2006. Unraveling the Gordian Knot: Interactions among vegetation, topography, and soil properties in the central and southern Appalachians. J. Torrey Bot. Soc. 133, 321–361. https://doi.org/10.3159/1https://doi.org/10.3159/1095-5674(2006)133[321:UTGKIA]2.0.CO;2

Brassard, B.W., Chen, H.Y.H., 2008. Effects of forest type and disturbance on diversity of coarse woody debris in boreal forest. Ecosystems 11, 1078–1090. https://doi.org/10.1007/s10021-008-9180-x

Buma, B., Pawlik, Ł., 2021. Post-landslide soil and vegetation recovery in a dry, montane system is slow and patchy. Ecosphere 12. https://doi.org/10.1002/ecs2.3346

Chang, C.-R., Lee, P.-F., Bai, M.-L., Lin, T.-T., 2006. Identifying the Scale Thresholds for Field-Data Extrapolation via Spatial Analysis of Landscape Gradients. Ecosystems 9, 200–214. https://doi.org/10.1007/s10021-005-0095-5

Dale, V.H., Joyce, L.A., McNulty, S., Neilson, R.P., Ayres, M.P., Flannigan, M.D., Hanson, P.J., Irland, L.C., Lugo, A.E., Peterson, C.J., Simberloff, D., Swanson, F.J., Stocks, B.J., Wotton, B.M., 2001. Climate Change and Forest Disturbances: Climate change can affect forests by altering the frequency, intensity, duration, and timing of fire, drought, introduced species, insect and pathogen outbreaks, hurricanes, windstorms, ice storms, or landslides. Bioscience 51, 723–734. https://doi.org/10.1641/0006-3568(2001)051[0723:CCAFD]2.0.CO;2

Forestry and Forest Products Research Institute, 2016. The methods of forest soil inventory Ver. 3 (1) The methods of field survey. Forestry and Forest Products Research Institute.

Fraver, S., Ringvall, A., Jonsson, B.G., 2007. Refining volume estimates of down woody debris. Can. J. For. Res. 37, 627–633. https://doi.org/10.1139/X06-269

Freund, C.A., Clark, K.E., Curran, J.F., Asner, G.P., Silman, M.R., 2021. Landslide age, elevation and residual vegetation determine tropical montane forest canopy recovery and biomass accumulation after landslide disturbances in the Peruvian Andes. J. Ecol. 1–17. https://doi.org/10.1111/1365-2745.13737

Fukasawa, Y., 2012. Effects of wood decomposer fungi on tree seedling establishment on coarse woody debris. For. Ecol. Manage. 266, 232–238. https://doi.org/10.1016/j.foreco.2011.11.027

Geological Survey of Japan, A., 2022. Seamless digital geological map of Japan V2 1: 200,000. [WWW Document]. URL https://gbank.gsj.jp/seamless (accessed 5.15.22).

Graham, R.L., Cromack, K., 1982. Mass, nutrient content, and decay rate of dead boles in rain forests of Olympic National Park. Can. J. For. Res. 12, 511–521. https://doi.org/10.1139/x82-080

Guariguata, M.R., 1990. Landslide Disturbance and Forest Regeneration in the Upper Luquillo Mountains of Puerto Rico. J. Ecol. 78, 814–832.

Hansen, E.M., Amacher, M.C., Van Miegroet, H., Long, J.N., Ryan, M.G., 2015. Carbon Dynamics in Central US Rockies Lodgepole Pine Type after Mountain Pine Beetle Outbreaks. For. Sci. 61, 665–679. https://doi.org/10.5849/forsci.14-094

Heilmann-Clausen, J., 2001. A gradient analysis of communities of macrofungi and slime moulds on decaying beech logs. Mycol. Res. 105, 575–596. https://doi.org/10.1017/S0953756201003665

Hind, N., Kay, J., 2006. A nature print of *Petasites Japonicus* subsp. *Giganteus*. Curtis's Bot. Mag. 23, 325–341. https://doi.org/10.1111/j.1467-8748.2006.00547.x

Hotta, W., Morimoto, J., Inoue, T., Suzuki, S.N., Umebayashi, T., Owari, T., Shibata, H., Ishibashi, S., Hara, T., Nakamura, F., 2020. Recovery and allocation of carbon stocks in boreal forests 64 years after catastrophic windthrow and salvage logging in northern Japan. For. Ecol. Manage. 468, 118169. https://doi.org/10.1016/j.foreco.2020.118169

IUSS Working Group WRB, 2015. World reference base for soil resources 2014, update 2015. International soil classification system for naming soils and creating legends for soil maps., World Soil Resources Reports. FAO, Rome.

Jager, M.M., Richardson, S.J., Bellingham, P.J., Clearwater, M.J., Laughlin, D.C., 2015. Soil fertility induces coordinated responses of multiple independent functional traits. J. Ecol. 103, 374–385. https://doi.org/10.1111/1365-2745.12366

Japan Meteorological Agency, 2022. Mesh Climate Data 2020 [WWW Document]. Natl. L. Numer. Inf. URL https://nlftp.mlit.go.jp/ksj/gml/datalist/KsjTmplt-G02-v3_0.html (accessed 5.5.22).

Johnstone, J.F., Allen, C.D., Franklin, J.F., Frelich, L.E., Harvey, B.J., Higuera, P.E., Mack, M.C., Meentemeyer, R.K., Metz, M.R., Perry, G.L.W., Schoennagel, T., Turner, M.G., 2016. Changing disturbance regimes, ecological memory, and forest resilience. Front. Ecol. Environ. 14, 369–378. https://doi.org/10.1002/fee.1311

Joshi, R.K., Garkoti, S.C., 2021. Dynamics of ecosystem carbon stocks in a chronosequence of nitrogen-fixing Nepalese alder (Alnus nepalensis D. Don.) forest stands in the central Himalayas. L. Degrad. Dev. 32, 4067–4086. https://doi.org/10.1002/ldr.3901

Jules, M.J., Sawyer, J.O., Jules, E.S., 2008. Assessing the relationships between stand development and understory vegetation using a 420-year chronosequence. For. Ecol. Manage. 255, 2384–2393. https://doi.org/10.1016/j.foreco.2007.12.042

Kita, K., 2018. An inventory of landslides triggered by Hokkaido Eastern Iburi earthquake, September 2018 [WWW Document]. URL https://koukita.github.io/2018_09_06_atumatyou/ (accessed 1.16.23).

Krankina, O.N., Harmon, M.E., 1995. Dynamics of the dead wood carbon pool in northwestern Russian boreal forests. Water, Air, Soil Pollut. 82, 227–238. https://doi.org/10.1007/BF01182836

Lal, R., 2004. Soil Carbon Sequestration Impacts on Global Climate Change and Food Security. Science 304, 1623–1627. https://doi.org/10.1126/science.1097396

Lateltin, O., Beer, C., Raetzo, H., Caron, C., 1997. Landslides in Flysch terranes of Switzerland: Causal factors and climate change. Eclogae Geol. Helv. 90, 401–406.

https://doi.org/https://doi.org/10.5169/seals-168171

Makita, A., Konno, Y., Fujita, N., Takada, K., Hamabata, E., 1993. Recovery of a Sasa tsuboiana population after mass flowering and death. Ecol. Res. 8, 215–224. https://doi.org/10.1007/BF02348534

Martínez-Murillo, J.F., Nadal-Romero, E., Regüés, D., Cerdà, A., Poesen, J., 2013. Soil erosion and hydrology of the western Mediterranean badlands throughout rainfall simulation experiments: A review. CATENA 106, 101–112. https://doi.org/10.1016/j.catena.2012.06.001

Martinez Arbizu, P., 2020. pairwiseAdonis: Pairwise multilevel comparison using adonis. R Package Version 0.4.

Murphy, S.J., Audino, L.D., Whitacre, J., Eck, J.L., Wenzel, J.W., Queenborough, S.A., Comita, L.S., 2015. Species associations structured by environment and land-use history promote beta-diversity in a temperate forest. Ecology 96, 705–715. https://doi.org/10.1890/14-0695.1

Oksanen, J., Simpson, G., Blanchet, F., Kindt, R., Legendre, P., Minchin, P., O'Hara, R., Solymos, P., Stevens, M., Szoecs, E., Wagner, H., Barbour, M., Bedward, M., Bolker, B., Borcard, D., Carvalho, G., Chirico, M., De Caceres, M., Durand, S., Evangelista, H., FitzJohn, R., Friendly, M., Furneaux, B., Hannigan, G., Hill, M., Lahti, L., McGlinn, D., Ouellette, M., Ribeiro Cunha, E., Smith, T., Stier, A., Ter Braak, C., Weedon, J., 2022. vegan: Community Ecology Package. R package version 2.6-4.

Pandey, A.N., Singh, J.S., 1985. Mechanism of ecosystem recovery: A case study from Kumaun, Himalaya. Reclam. Reveg. Res. 3, 271–292.

Prosser, I.P., Hughes, A.O., Rutherfurd, I.D., 2000. Bank erosion of an incised upland channel by subaerial processes: Tasmania, Australia. Earth Surf. Process. Landforms 25, 1085–1101. https://doi.org/10.1002/1096-9837(200009)25:10<1085::AID-ESP118>3.0.CO;2-K

QGIS Development Team, 2021. QGIS geographic information system [WWW Document]. Open source geospatial Found. Proj. URL http://qgis.osgeo.org. (accessed 3.9.23).

R Core Team, 2022. R: A language and environment for statistical computing.

Reddy, V.S., Singh, J.S., 1993. Changes in Vegetation and Soil During Succession Following Landslide Disturbance in the Central Himalaya. J. Environ. Manage. 39, 235–250.

Reich, P.B., Tjoelker, M.G., Walters, M.B., Vanderklein, D.W., Buschena, C., 1998. Close association of RGR, leaf and root morphology, seed mass and shade tolerance in seedlings of nine boreal tree species grown in high and low light. Funct. Ecol. 12, 327–338. https://doi.org/10.1046/j.1365-2435.1998.00208.x

Restrepo, C., Vitousek, P., Neville, P., 2003. Landslides significantly alter land cover and the distribution of biomass: An example from the Ninole ridges of Hawai’i. Plant Ecol. 166, 131–143. https://doi.org/10.1023/A:1023225419111

Restrepo, C., Walker, L.R., Shiels, A.B., Bussmann, R., Claessens, L., Fisch, S., Lozano, P., Negi, G., Paolini, L., Poveda, G., Ramos-Scharrón, C., Richter, M., Velázquez, E., 2009. Landsliding and its multiscale influence on mountainscapes. Bioscience 59, 685–698. https://doi.org/10.1525/bio.2009.59.8.10

Rothstein, D.E., Yermakov, Z., Buell, A.L., 2004. Loss and recovery of ecosystem carbon pools following stand-replacing wildfire in Michigan jack pine forests. Can. J. For. Res. 34, 1908–1918. https://doi.org/10.1139/x04-063

Sato, H., Ishimaru, S., Kawakami, G., Kanno, M., Nagasaka, A., Abe, T., Tsushima, T., Tajika, J., 2013. Factors of shallow landslide caused by typhoon0310（Etau）in Appetsu River basin, Hidaka region, Hokkaido. J. Japan Soc. Eros. Control Eng. 66, 40-47 (in Japanese). https://doi.org/https://doi.org/10.11475/sabo.66.2_40

Schomakers, J., Jien, S., Lee, T., Huang, J., Hseu, Z., Liang, Z., Lee, L., Hein, T., Mentler, A., Zehetner, F., 2017. Soil and biomass carbon re-accumulation after landslide disturbances. Geomorphology 288, 164–174. https://doi.org/10.1016/j.geomorph.2017.03.032

Seedre, M., Taylor, A.R., Brassard, B.W., Chen, H.Y.H., Jõgiste, K., 2014. Recovery of Ecosystem Carbon Stocks in Young Boreal Forests: A Comparison of Harvesting and Wildfire Disturbance. Ecosystems 17, 851–863. https://doi.org/10.1007/s10021-014-9763-7

Shiels, A.B., West, C.A., Weiss, L., Klawinski, P.D., Walker, L.R., 2008. Soil factors predict initial plant colonization on Puerto Rican landslides. Plant Ecol. 165–178. https://doi.org/10.1007/s11258-007-9313-x

Spies, T.A., Franklin, J.F., Thomas, T.B., 1988. Coarse woody debris in Douglas-fir forests of western Oregon and Washington. Ecology 69, 1689–1702. https://doi.org/10.2307/1941147

Suchar, V.A., Crookston, N.L., 2010. Understory cover and biomass indices predictions for forest ecosystems of the Northwestern United States. Ecol. Indic. 10, 602–609. https://doi.org/10.1016/j.ecolind.2009.10.004

Vitousek, P., Howarth, R., 1991. Nitrogen limitation on land and in the sea: How can it occur? Biogeochemistry 13, 87–115. https://doi.org/10.1007/BF00002772

Walker, L.R., Velázquez, E., Shiels, A.B., 2009. Applying lessons from ecological succession to the restoration of landslides. Plant Soil 324, 157–168. https://doi.org/10.1007/s11104-008-9864-1

Wang, H., Saigusa, N., Yamamoto, S., Kondo, H., Hirano, T., Toriyama, A., Fujinuma, Y., 2004. Net ecosystem CO2 exchange over a larch forest in Hokkaido, Japan. Atmos. Environ. 38, 7021–7032. https://doi.org/10.1016/j.atmosenv.2004.02.071

Warrington, D., Shainberg, I., Agassi, M., Morin, J., 1989. Slope and Phosphogypsum's Effects on Runoff and Erosion. Soil Sci. Soc. Am. J. 53, 1201–1205. https://doi.org/10.2136/sssaj1989.03615995005300040035x

Wilcke, W., Valladarez, H., Stoyan, R., Yasin, S., Valarezo, C., Zech, W., 2003. Soil properties on a chronosequence of landslides in montane rain forest, Ecuador. CATENA 53, 79–95. https://doi.org/10.1016/S0341-8162(02)00196-0

Yanai, S., Igarashi, Y., 1990. History of the slope failure and paleoenvironment on the marine terrace of Hidaka district, central Hokkaido. Quat. Res. 29, 319-336 (in Japanese). https://doi.org/10.4116/jaqua.29.319

Yoda, K., Kira, H., Ogawa, H., Hozumi, K., 1963. Self-thinning in overcrowded pure stands under cultivated and natural conditions. J. Biol. Osaka City Univ. 14, 107–129.

Zhang, Q., Liang, Y., 1995. Effects of gap size on nutrient release from plant litter decomposition in a natural forest ecosystem. Can. J. For. Res. 25, 1627–1638. https://doi.org/10.1139/x95-177

TABLES

Table 1

(a) Slope angle (°)

Zone	Landslide age									
	3		18		40		74≤		Reference	
	Mean ± SE	n	Mean ± SE	n	Mean ± SE	n	Mean ± SE	n	Mean ± SE	n
Initiation/Upper	29.05 ± 1.34 ^{abA}	20	32.85 ± 1.59 ^{aA}	20	28.45 ± 0.64 ^{abA}	20	32.80 ± 0.98 ^{aA}	20	25.75 ± 1.45 ^{bA}	12
Transport/Middle	18.90 ± 1.05 ^{bB}	20	24.05 ± 1.08 ^{abB}	20	23.35 ± 1.58 ^{abA}	20	29.10 ± 0.94 ^{aA}	20	28.17 ± 0.79 ^{aA}	12
Deposition/Lower	7.90 ± 1.55 ^{bC}	20	16.50 ± 1.24 ^{aC}	20	14.85 ± 1.84 ^{aB}	20	NA	NA	11.33 ± 3.06 ^{abB}	12

(b) O layer depth (cm)

Initiation/Upper	0.00 ± 0.00 ^{bA}	20	0.30 ± 0.18 ^{bB}	20	4.65 ± 0.41 ^{aA}	20	6.63 ± 0.85 ^{aA}	20	6.58 ± 0.57 ^{aA}	12
Transport/Middle	0.00 ± 0.00 ^{cA}	20	1.15 ± 0.44 ^{bA}	20	5.55 ± 0.28 ^{aA}	20	7.65 ± 0.40 ^{aA}	20	6.17 ± 0.58 ^{aA}	12
Deposition/Lower	0.00 ± 0.00 ^{cA}	20	1.80 ± 0.42 ^{bA}	20	5.00 ± 0.49 ^{aA}	20	NA	NA	6.00 ± 0.58 ^{aA}	12

(c) Soil moisture content (%)

Initiation/Upper	8.70 ± 0.49 ^{aB}	20	13.94 ± 1.28 ^{aA}	20	12.56 ± 0.89 ^{aB}	20	10.78 ± 0.92 ^{aA}	20	13.85 ± 0.75 ^{aA}	12
Transport/Middle	16.34 ± 0.96 ^{aA}	20	16.90 ± 1.93 ^{aA}	20	19.10 ± 2.33 ^{aAB}	20	12.23 ± 1.02 ^{aA}	20	16.77 ± 1.10 ^{aA}	12
Deposition/Lower	14.38 ± 0.68 ^{aA}	20	18.90 ± 1.77 ^{aA}	20	20.58 ± 2.57 ^{aA}	20	NA	NA	20.13 ± 1.95 ^{aA}	12

Table 2

Zone	Live trees AGB (Mg ha^{-1})		Understory vegetation biomass index (m^{-2})		CWD (Mg ha^{-1})		Surface soils carbon stock (MgC ha^{-1})		Surface soils nitrogen stock (MgN ha^{-1})	
	Mean ± SE	n	Mean ± SE	n	Mean ± SE	n	Mean ± SE	n	Mean ± SE	n
Initiation	0.00 ± 0.00 ^{A}	5	1.35 ± 0.32 ^{C}	20	0.00 ± 0.00 ^{B}	5	5.25 ± 1.53 ^{A}	5	0.53 ± 0.13 ^{A}	5
Transport	0.00 ± 0.00 ^{A}	5	3.61 ± 0.47 ^{B}	20	3.71 ± 2.54 ^{B}	5	3.31 ± 0.76 ^{A}	5	0.71 ± 0.08 ^{A}	5
Deposition	0.00 ± 0.00 ^{A}	5	19.86 ± 2.81 ^{A}	20	14.12 ± 4.54 ^{A}	5	4.37 ± 1.06 ^{A}	5	0.47 ± 0.08 ^{A}	5

FIGURES

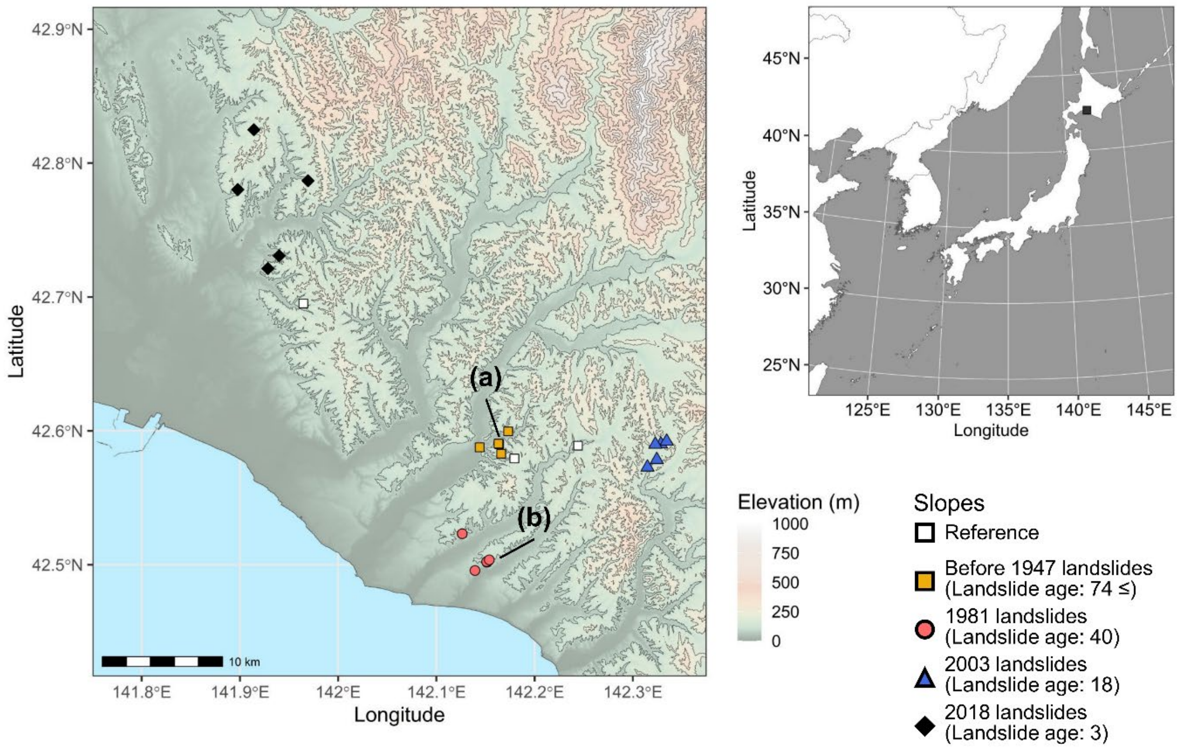

Fig. 1

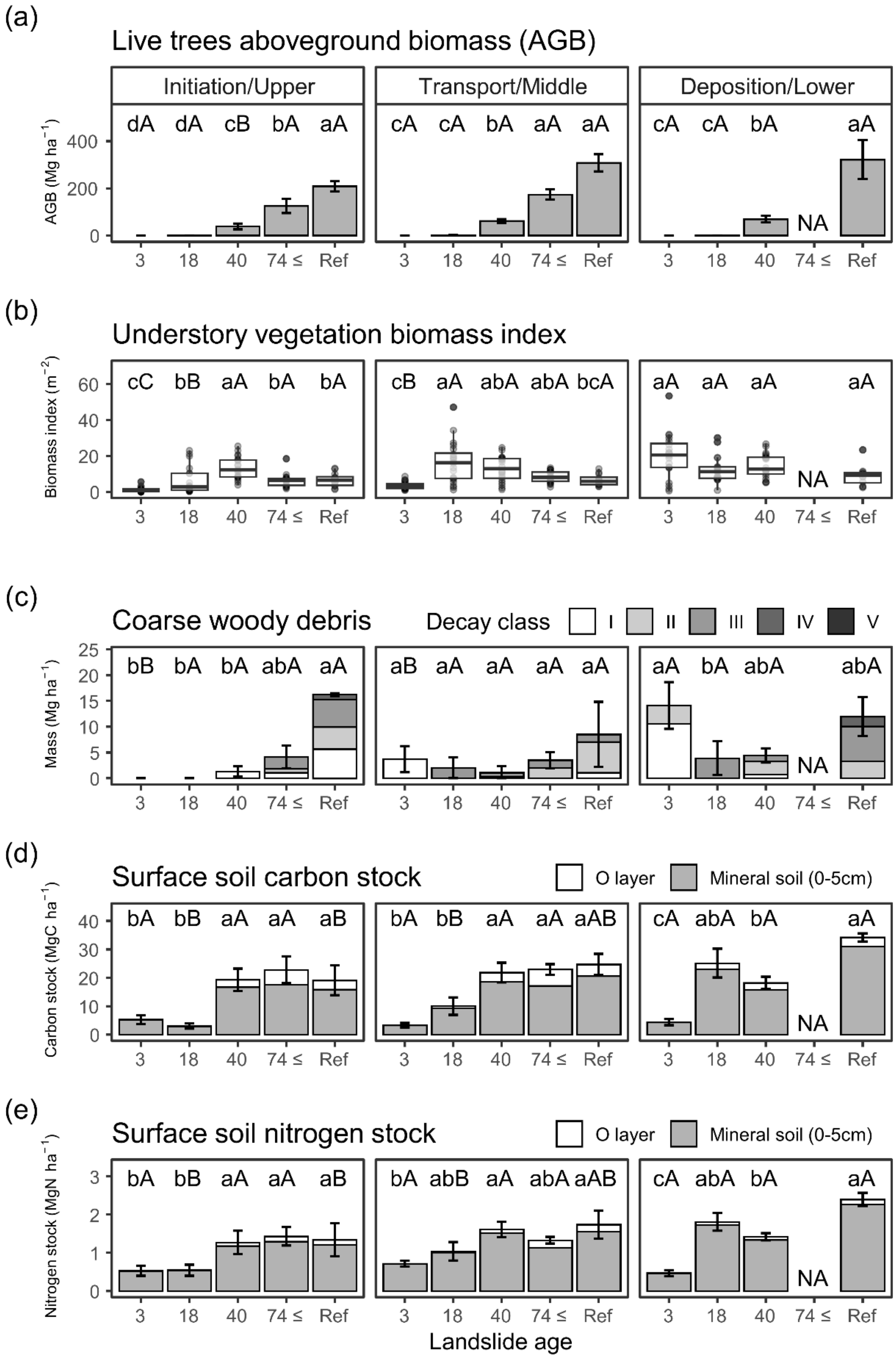
(a)
Live trees aboveground biomass (AGB)
Initiation/Upper
Transport/Middle
Deposition/Lower
AGB (Mg ha⁻¹)
NA
(b)
Understory vegetation biomass index
Biomass index (m⁻²)
(c)
Coarse woody debris
Decay class I II III IV V
Mass (Mg ha⁻¹)
(d)
Surface soil carbon stock
O layer
Mineral soil (0-5cm)
Carbon stock (MgC ha⁻¹)
(e)
Surface soil nitrogen stock
Nitrogen stock (MgN ha⁻¹)
3 18 40 74 ≤ Ref
Landslide age

Fig. 2

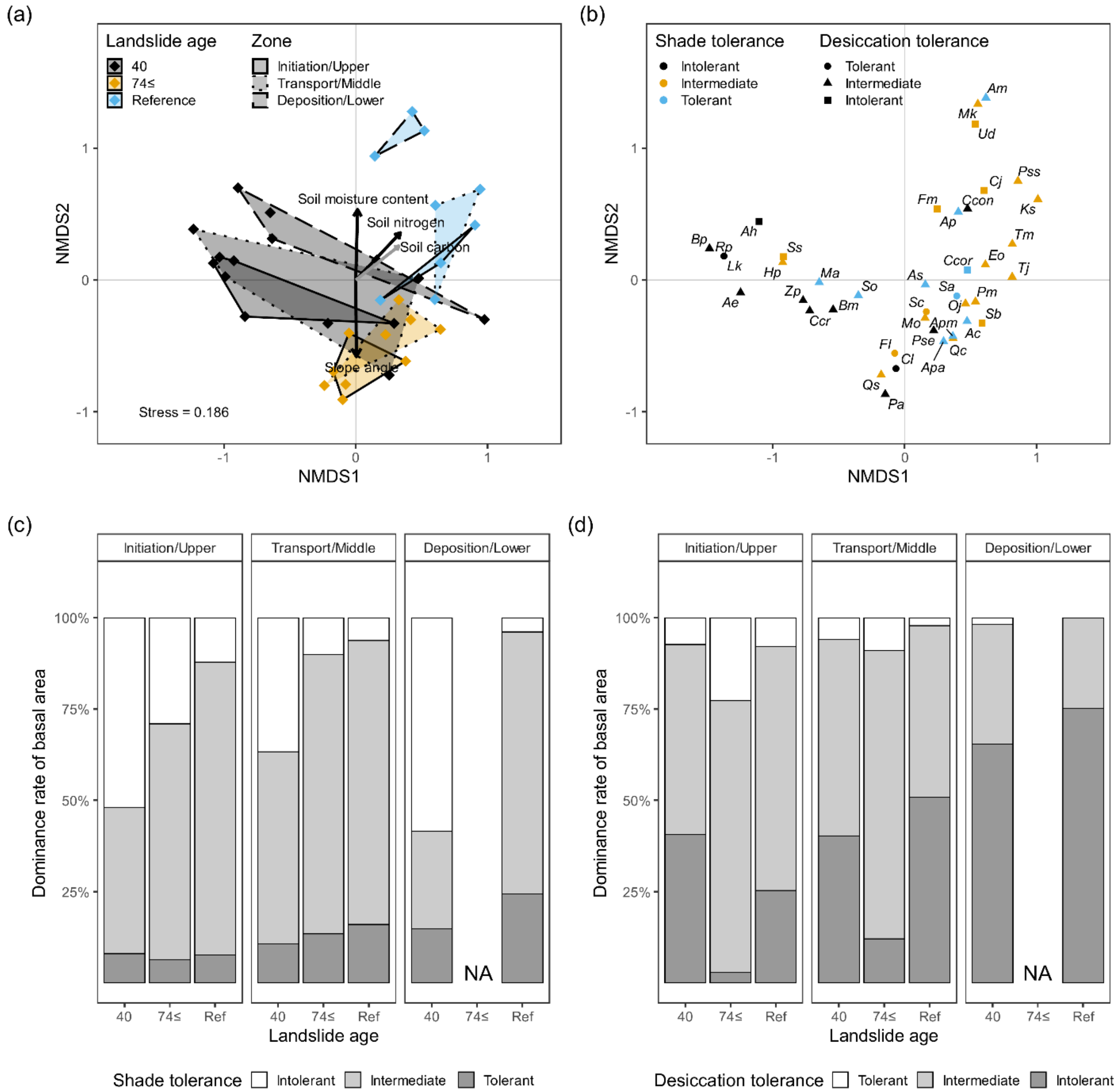
(a)
Landslide age
40
74≤
Reference
Zone
Initiation/Upper
Transport/Middle
Deposition/Lower
Soil moisture content
Soil nitrogen
Soil carbon
Slope angle
Stress = 0.186
NMDS1
NMDS2
(b)
Shade tolerance
Intolerant
Intermediate
Tolerant
Desiccation tolerance
Tolerant
Intermediate
Intolerant
NMDS1
NMDS2
(c)
Initiation/Upper
Transport/Middle
Deposition/Lower
Dominance rate of basal area
NA
Landslide age
Shade tolerance
Intolerant
Intermediate
Tolerant
(d)
Initiation/Upper
Transport/Middle
Deposition/Lower
Dominance rate of basal area
NA
Landslide age
Desiccation tolerance
Tolerant
Intermediate
Intolerant

Fig. 3

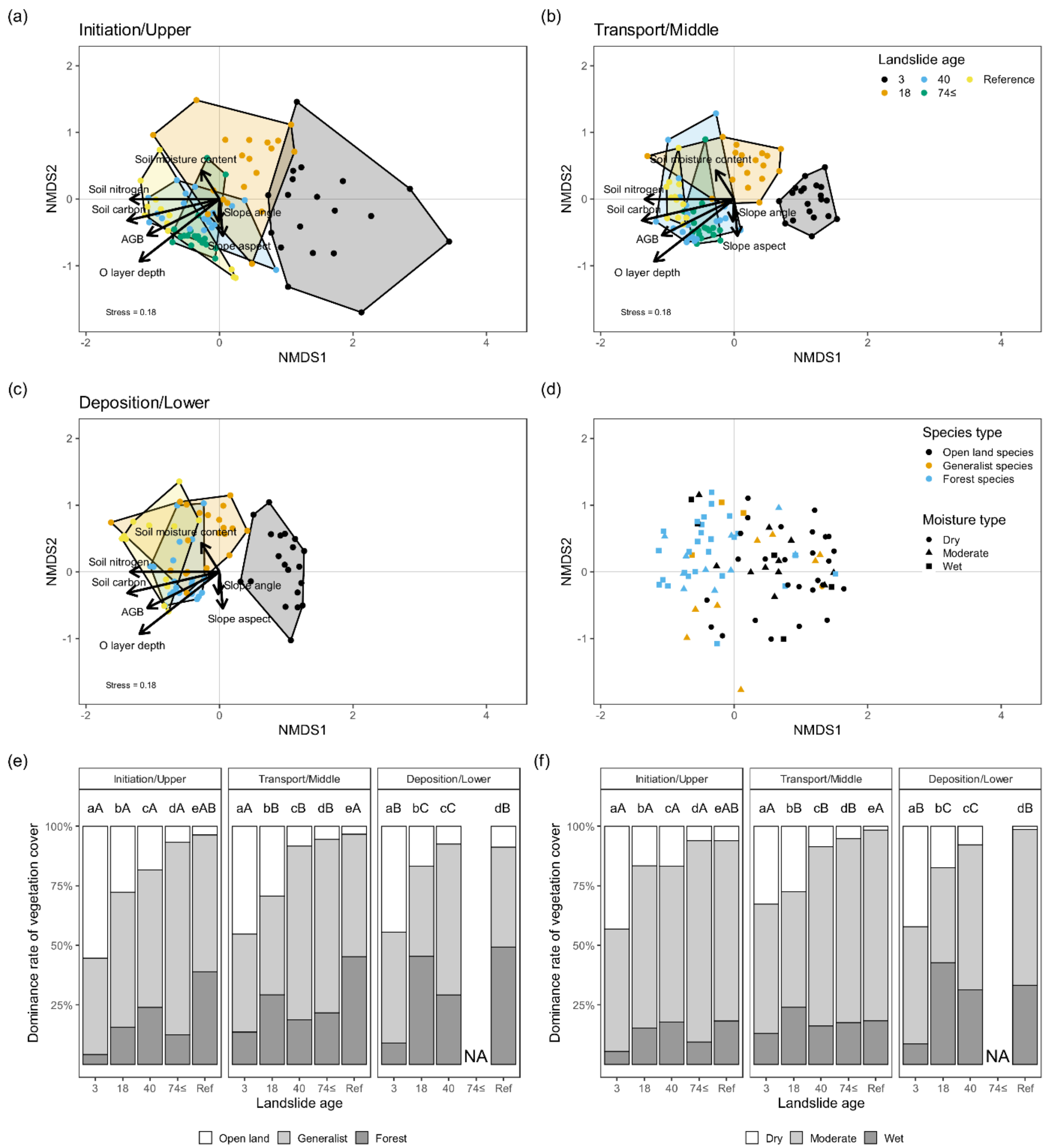
(a)
Initiation/Upper
Soil moisture content
Soil nitrogen
Soil carbon
Slope angle
AGB
Slope aspect
O layer depth
Stress = 0.18
NMDS1
NMDS2
(b)
Transport/Middle
Landslide age
3
40
Reference
18
74≤
(c)
Deposition/Lower
(d)
Species type
Open land species
Generalist species
Forest species
Moisture type
Dry
Moderate
Wet
(e)
Initiation/Upper
Transport/Middle
Deposition/Lower
aA bA cA dA eAB
aA bB cB dB eA
aB bC cC dB
NA
Dominance rate of vegetation cover
Landslide age
Open land
Generalist
Forest
(f)
aA bA cA dA eAB
aA bB cB dB eA
aB bC cC dB
Dry
Moderate
Wet

737 **Fig. 4**

738

TABLE CAPTIONS

Table 1 Characteristics of studied landslides based on slope angle, O layer depth, and soil moisture content.

Different lowercase letters next to the values indicate significant differences between landslide ages within each zone ($p < 0.05$) according to multiple comparisons. Different capital letters next to the values indicate significant differences between zones within each landslide age ($p < 0.05$) according to multiple comparisons.

Table 2 Ecosystem attributes in three-year old landslides.

Different capital letters next to the values indicate significant differences in the amount of each forest ecosystem component among the zones ($p < 0.05$) according to multiple comparisons. AGB: aboveground biomass; CWD: coarse woody debris.

FIGURE CAPTIONS

Fig. 1 Map of the study area.

Right: Map of northern Japan and its surroundings. The black rectangle indicates the range of the detailed map on the left. Left: The detailed map of the study area. The points indicate the location of the study landslides and slopes. (a) Two slopes where landslides occurred before 1947. (b) Three slopes where landslides occurred in 1981.

Fig. 2 Chronological changes in each forest ecosystem component in each slope zone.

The chronological changes in (a) live tree AGB, (b) the biomass indices of understory vegetation, (c) coarse woody debris (CWD) mass, (d) surface soil carbon stock, and (e) surface soil nitrogen stock in each slope zone. Error bars in (a), (c), (d), and (e) indicate standard errors of each forest ecosystem component of each combination of landslide age and zone. Colors in (c) indicate decay classes. White and gray bars in (d) and (e) indicate the O layer and mineral soil, respectively. Different lowercase letters above the bars indicate significant differences between landslide ages within each zone ($p < 0.05$) according to multiple comparisons. Different capital letters above the bars indicate significant differences between zones within each landslide age ($p < 0.05$) according to multiple comparisons. The data for landslide age 3 are the same data shown in Table 2.

Fig. 3 Live tree species composition based on basal area.

Ordination analysis (NMDS) of live trees for (a) plots and environmental variables (only significant ($p < 0.05$) and marginally significant ($p < 0.10$) variables are shown) and for (b) species. Colors and line types in (a) indicate landslide ages and zones, respectively. Arrows in (a) indicate the directions of the greatest environmental gradient of each environmental variable (black: $p < 0.05$; gray: $p < 0.10$). Colors and point shapes in (b) indicate species shade tolerance and desiccation tolerance, respectively. For full species names, please see Table S3. (c) Dominance rate of basal area classified by shade tolerance. (d) Dominance rate of the basal area classified by desiccation tolerance.

Fig. 4 Understory vegetation species composition based on vegetation cover.

NMDS results of understory vegetation for (a) quadrats in the initiation/upper zone, (b) quadrats in the transport/middle zone, (c) quadrats in the deposition/lower zone, and (d) species (only herbaceous species are shown). Arrows in (a), (b), and (c) indicate the directions of the greatest environmental gradient of each environmental variable (only significant variables ($p < 0.05$) are shown). Notably, the same ordination result is divided and displayed by zone in (a), (b), and (c). The colors in (a), (b), and (c) indicate landslide age. Colors and point shapes in (d) indicate species type and moisture type, respectively. (e) Dominance rate of herbaceous species vegetation cover classified by species type. (f) Dominance rate of herbaceous species vegetation cover classified by moisture type. Different lowercase letters above the bars indicate significant differences in species composition between landslide ages within each zone ($p < 0.05$) according to PERMANOVA and multiple comparisons. Different capital letters above the bars indicate significant differences in species composition between zones within each landslide age ($p < 0.05$) according to PERMANOVA and multiple comparisons.